NASA/TM-20240015672

Multiscale Modeling of Thermoplastics Using Atomistic-Informed Micromechanics

Evan J. Pineda
Glenn Research Center, Cleveland, Ohio

Jamal F. Husseini
University of Massachusetts, Lowell, Massachusetts

Joshua D. Kemppainen
Michigan Technological University, Houghton, Michigan

Brett A. Bednarcyk
Glenn Research Center, Cleveland, Ohio

William A. Pisani
U.S. Army Engineer Research and Development Center, Vicksburg, Mississippi

Gregory M. Odegard
Michigan Technological University, Houghton, Michigan

Scott E. Stapleton
University of Massachusetts, Lowell, Massachusetts

December 2024

NASA STI Program Report Series

Since its founding, NASA has been dedicated to the advancement of aeronautics and space science. The NASA scientific and technical information (STI) program plays a key part in helping NASA maintain this important role.

The NASA STI program operates under the auspices of the Agency Chief Information Officer. It collects, organizes, provides for archiving, and disseminates NASA's STI. The NASA STI program provides access to the NTRS Registered and its public interface, the NASA Technical Reports Server, thus providing one of the largest collections of aeronautical and space science STI in the world. Results are published in both non-NASA channels and by NASA in the NASA STI Report Series, which includes the following report types:

- TECHNICAL PUBLICATION.
  Reports of completed research or a major significant phase of research that present the results of NASA programs and include extensive data or theoretical analysis. Includes compilations of significant scientific and technical data and information deemed to be of continuing reference value. NASA counterpart of peer-reviewed formal professional papers but has less stringent limitations on manuscript length and extent of graphic presentations.

- TECHNICAL MEMORANDUM.
  Scientific and technical findings that are preliminary or of specialized interest, e.g., quick release reports, working papers, and bibliographies that contain minimal annotation. Does not contain extensive analysis.

- CONTRACTOR REPORT.
  Scientific and technical findings by NASA-sponsored contractors and grantees.

- CONFERENCE PUBLICATION.
  Collected papers from scientific and technical conferences, symposia, seminars, or other meetings sponsored or cosponsored by NASA.

- SPECIAL PUBLICATION.
  Scientific, technical, or historical information from NASA programs, projects, and missions, often concerned with subjects having substantial public interest.

- TECHNICAL TRANSLATION.
  English-language translations of foreign scientific and technical material pertinent to NASA's mission.

Specialized services also include organizing and publishing research results, distributing specialized research announcements and feeds, providing information desk and personal search support, and enabling data exchange services.

For more information about the NASA STI program, see the following:

- Access the NASA STI program home page at http://www.sti.nasa.gov

NASA/TM-20240015672

Multiscale Modeling of Thermoplastics Using Atomistic-Informed Micromechanics

Evan J. Pineda
Glenn Research Center, Cleveland, Ohio

Jamal F. Husseini
University of Massachusetts, Lowell, Massachusetts

Joshua D. Kemppainen
Michigan Technological University, Houghton, Michigan

Brett A. Bednarcyk
Glenn Research Center, Cleveland, Ohio

William A. Pisani
U.S. Army Engineer Research and Development Center, Vicksburg, Mississippi

Gregory M. Odegard
Michigan Technological University, Houghton, Michigan

Scott E. Stapleton
University of Massachusetts, Lowell, Massachusetts

National Aeronautics and
Space Administration

Glenn Research Center
Cleveland, Ohio 44135

December 2024

Acknowledgments

Dr. Pineda's contributions were sponsored by the Office of Naval Research (ONR) under Interagency Agreement SAA3-1697. Mr. Husseini's contributions were funded by a NASA Space Technology Graduate Research Opportunity (NSTGRO) Grant Number #80NSSC21K1285. Dr. Bednarcyk would like to thank the NASA Thermoplastics Development for Exploration Applications (TDEA) project for their support. Mr. Kemppainen would like to acknowledge the NASA Internship Project (NIP).

Level of Review: This material has been technically reviewed by technical management.

This report is available in electronic form at https://www.sti.nasa.gov/ and https://ntrs.nasa.gov/

NASA STI Program/Mail Stop 050
NASA Langley Research Center
Hampton, VA 23681-2199

Multiscale Modeling of Thermoplastics Using Atomistic-Informed Micromechanics

Evan J. Pineda
National Aeronautics and Space Administration
Glenn Research Center
Cleveland, Ohio 44135

Jamal F. Husseini
University of Massachusetts
Lowell, Massachusetts 01854

Joshua D. Kemppainen
Michigan Technological University
Houghton, Michigan 49931

Brett A. Bednarcyk
National Aeronautics and Space Administration
Glenn Research Center
Cleveland, Ohio 44135

William A. Pisani
U.S. Army Engineer Research and Development Center
Vicksburg, Mississippi 39180

Gregory M. Odegard
Michigan Technological University
Houghton, Michigan 49931

Scott E. Stapleton
University of Massachusetts
Lowell, Massachusetts 01854

Abstract

A multiscale repeating unit cell model of a single spherulite containing four disparate length scales was developed to predict the thermoelastic behavior of semicrystalline thermoplastic materials for composite aerospace applications. The continuum level scales were fully coupled and modeled using the generalized method of cells and the high fidelity generalized method of cells micromechanics theories. Data from molecular dynamics simulations were used as inputs for the amorphous and crystalline constituents in the multiscale continuum models. Effective Young's modulus, shear modulus, Poisson's ratio, coefficient of thermal expansion, and thermal conductivity were predicted for polyether ether ketone and polyether ketone ketone, showing good agreement with the available experimental data from the open literature. Moreover, it is shown that predicted properties are fairly insensitive to the fidelity of the micromechanics model used at the highest continuum scale or the assumed shape of the spherulite.

1.0 Introduction

Thermoplastic materials, including polyether ether ketone (PEEK) and polyether ketone ketone (PEKK) are high-performance semicrystalline polymers used in aerospace applications because of their excellent properties including toughness, resistance to aging, and manufacturability. The increased interest in these materials is evident by several recently established NASA projects that focus on the use of thermoplastic composites for both aeronautics and space applications. The resulting crystallinity in a neat semicrystalline thermoplastic or thermoplastic composite is a result of the processing conditions (i.e., time and temperature) and has a significant influence on the thermomechanical properties. For example, there is about a 30 percent measured difference between the Young's modulus of amorphous PEEK and fully crystallized PEEK (Ref. 1). This is a product of the highly directional properties of the thermoplastic crystallites, as compared to the isotropic amorphous phase. Moreover, the radius of the spherulites is relatively large, on the order of that of a carbon fiber, and the semicrystalline morphological structure of the spherulites are quite complex and contain sever relevant length scale. Finally, the presence of carbon fibers in a thermoplastic composite can heavily influence the crystallization kinetics and final microstructure in the matrix. To design improved composite matrix materials incorporating thermoplastics, a thorough understanding of the coupling between the molecular structure, continuum-level microstructure, and the resulting bulk response of the thermoplastics is imperative.

A recent review paper collected information on the morphology of neat PEEK and PEKK near a carbon fiber interface and the influence of crystallinity on Young's modulus (Ref. 1). Wherever relevant, comparisons of PEKK to the more extensively studied PEEK were drawn. Talbott et al. demonstrated experimentally that Young's modulus, shear modulus, tensile yield strength, and shear yield strength increase as the relative crystalline content of PEEK increases (Ref. 2). More recently, similar measurements have been made for PEKK (Ref. 3). Despite these initial efforts, more experimental research is needed to provide a better understanding of the effect of molecular structure on bulk properties of PEKK and PEEK.

Computational simulation techniques can also be used to establish structure-property relationships for thermoplastic materials and supplement experimental data. Specifically, molecular dynamics (MD) simulation techniques are well-suited for predicting bulk-level properties of single-phase polymers based on molecular structure (Refs. 4 and 5). However, MD simulation techniques alone cannot predict the bulk level properties of semicrystalline materials because the characteristic length scales (i.e., crystallites, granular crystalline blocks (GCBs), lamellae, spherulites) of these materials (microns) is orders of magnitude larger than those that can be tractably simulated with MD models (nanometers).

An early multiscale model for thermoplastic composites was presented by Chapman et al. to examine residual stresses in carbon/PEEK laminates (Ref. 6). At the crystalline/amorphous scale in the PEEK matrix, this work employed the micromechanics model of Ogale and McCullough, which considered the aspect ratio and a random orientation of the crystalline phase (Ref. 7). Based on these homogenized PEEK matrix properties, Chapman et al. (Ref. 6) then used rule of mixtures type models for the unidirectional ply (including viscoelastic effects in the transverse direction) and lamination theory to obtain the macroscale laminate thermo-mechanical response. In more recent years, there have been several analytical micromechanics models presented in the literature for predicting the properties and response of semicrystalline thermoplastics based on the properties of the amorphous and crystalline constituent phases. For example, Guan and Pitchumani used an ellipsoidal Mori-Tanaka micromechanics model to predict the Young's moduli of semicrystalline polyethylene and syndiotactic polystyrene as a function of crystallinity (Ref. 8). Their results showed the importance of capturing the semicrystalline microstructure for predicting accurate elastic properties. Bédoui and co-workers used several classical

micromechanics homogenization methods to predict the effective elastic properties of semicrystalline isotactic polypropylene, polyethylene, and polyethylene terephthalate (PET) (Ref. 9). They then extended this investigation to consider the viscoelastic behavior of PET (Ref. 10). Gueguen et al. compared Mori-Tanaka, double-inclusion, and self-consistent micromechanics models for predicting the elastic properties of semicrystalline polyethylene based on the amorphous and crystalline phases (Ref. 11). Glüge et al. used an uncoupled, two-step homogenization approach, including orientational averaging, to predict the effective Young's modulus of semicrystalline isotactic polypropylene as a function of crystallinity (Ref. 12). van Dommelen et al. extended existing micromechanics methods to include viscoplasticity and large deformations to investigate the response of high-density polyethylene and PET (Ref. 13).

The literature indicates that more emphasis has been placed on analytical and semi-analytical micromechanics models for semicrystalline thermoplastics as opposed to numerical, finite element method (FEM) models. Examples of FEM-based micromechanics models for semicrystalline thermoplastics include the work of Hsia et al. (Ref. 14), Doyle (Ref. 15), and Poluektov (Ref. 16). Of course, this approach requires meshing of the microstructure and tends to be more computationally demanding, particularly when considering multiple scales. Finally, Jin et al. (Ref. 17), in addition to presenting a comprehensive investigation of PEEK semicrystalline microstructure, developed a relevant MD model of the crystalline phase that incorporated imperfections.

To simulate semicrystalline polymer materials effectively, a multiscale approach can be used in which the amorphous and crystalline phases are modeled separately using MD, and multiscale micromechanics is subsequently used to obtain the bulk properties using repeating unit cells (RUCs) that represent the spatial, and hierarchical, arrangement of these phases at larger length scales. An integrated framework allows for engineers both to design with the material and design the material itself. It has been demonstrated previously that MD modeling coupled hierarchically with the multiscale generalized method of cells (MsGMC) can be used to accurately predict the mechanical properties of semicrystalline PEEK (Refs. 18 and 19). These papers presented the methodology for establishing well-equilibrated amorphous and crystalline PEEK MD models with the Reactive Force Field (ReaxFF) (Ref. 20), as well as the procedure for predicting the mechanical response of each phase at the molecular level. The crystalline PEEK MD results were compared with density functional theory (DFT) results for validation. This study also presented the methodology for modeling the semicrystalline structure of PEEK with the MsGMC module of the NASA Micromechanics Analysis Code/Generalized Method of Cells (MAC/GMC) using the simulated molecular response as input (Refs. 21 and 22). Following this, the predicted mechanical properties were compared to experiment for model validation for one value of crystallinity. The multiscale modeling methodology was later extended to semicrystalline polyamide 6 (Ref. 23).

The multiscale continuum model for the semicrystalline spherulite has been further matured using the multiscale recursive micromechanics (MsRM) framework within the NASA Multiscale Analysis Tool (NASMAT, https://software.nasa.gov/software/LEW-20244-1) software package developed at the NASA Glenn Research Center (Refs. 24 and 25). The MsRM framework within NASMAT offers more flexibility than MsGMC in MAC/GMC because it allows for any micromechanics theory to be deployed at any scale in an integrated manner, i.e., two-way coupling including homogenization and de-homogenization, or localization. Thus, the high fidelity generalized method of cells (HFGMC) can be utilized at the highest scale to capture the local fields arising from the presence of a spherical inclusion more accurately, but at an increased computational cost, while the generalized method of cells (GMC) can be retained for all additional subscales. Moreover, the original MsGMC model for PEEK utilized a cubic shape for the spherulite. With GMC, the sharp corners of the cubic inclusion do not influence the local fields. However, these stress concentrations are captured with HFGMC. Therefore, a more realistic,

spherical model for the spherulite was also generated. Finally, to predict the effective thermal conductivity of semicrystalline materials, a generalized HFGMC solution for physics governed by vector-based constitutive laws has been implemented into MsRM within NASMAT (Ref. 26). The inputs for the crystalline and amorphous phase properties are obtained from MD results from Pisani, et al. (PEEK), and more recently, Kemppainen et al. (PEKK) (Refs. 18 and 27). The work presented here represents a purely computational workflow for predicting effective thermoelastic properties as a function of crystallinity, and it is validated against experimental data where available.

The focus of the current work is to evaluate the different MsRM modeling strategies for their ability to predictive effective thermoelastic properties of semicrystalline thermoplastics. As such, it is also important to understand modeling requirements, theoretical restrictions, and computational performance of the models. The current paper is arranged as follows. A summary of the HFGMC homogenization for physics governed by vectorized constitutive laws is given in Section 2.0. Details on the MsRM model for the spherulite are given in Section 3.0. The predicted stiffness, coefficient of thermal expansion (CTE), and thermal conductivity properties for PEEK and PEKK, as a function of crystallinity, are presented in Section 4.0, followed by conclusions in Section 5.0.

2.0 Generalized HFGMC Solution for Physics Governed by Vector-Based Constitutive Laws

A new version of the HFGMC micromechanics theory was formulated for many different physical phenomena governed by vector constitutive laws, such as heat transfer, in Bednarcyk, et al. in composite materials (Ref. 26). The second-order temperature (or potential) field used in HFGMC provides coupling that is absent in GMC, which is first-order. This enables, for example, the more physical redistribution among the heat flux components as the heat flow follows its natural, often tortuous, path through the microstructure of a material. For the classical formulations of GMC and HFGMC, the reader is referred to Aboudi et al. (Ref. 22). This enabled, in addition to the standard mechanical problem, (1) homogenization to obtain effective composite properties and (2) localization to obtain local field quantities for thermal and electrical conductivity problems, magnetic permeability problems, diffusion problems, and problems involving fluid flow through a porous medium. The constitutive equations for all these physical phenomena can be written in a common form as,

$$\mathbf{Y} = -\mathbf{Z}\nabla\psi = \mathbf{Z}\,\mathbf{X} \tag{1}$$

where, for example, in the case of the thermal conductivity problem, this represents Fourier's Law,

$$\mathbf{q} = -\boldsymbol{\kappa}\nabla T \tag{2}$$

where $\mathbf{q}$ is the heat flux vector, $\boldsymbol{\kappa}$ is the second-order thermal conductivity tensor, and T is the temperature, so,

$$\mathbf{Y} = \mathbf{q}, \qquad \psi = T, \qquad \mathbf{Z} = \boldsymbol{\kappa}, \qquad \mathbf{X} = -\nabla T \tag{3}$$

Similar analogies can be made for all the physics described above, and, by simply using the correct input properties for the constituent materials, the effective composite properties associated with any of the physics can be determined via the HFGMC homogenization procedure. Likewise, by considering application of the appropriate global field quantities (for example, global composite heat fluxes), the local

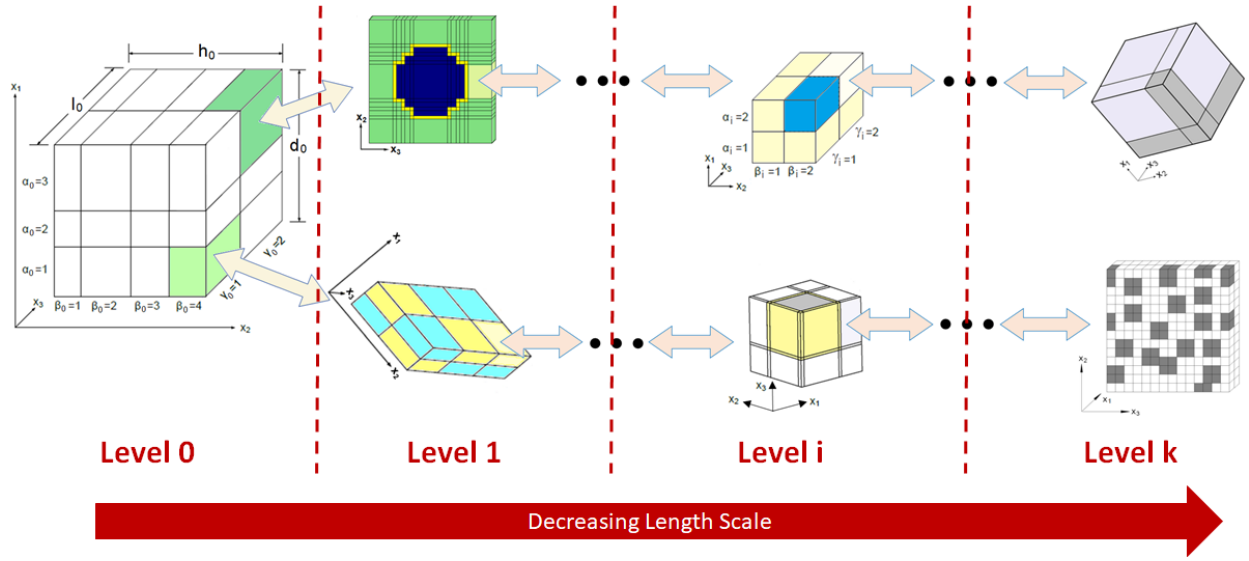

Figure 1.—MsRM integrated hierarchy linking repeating unit cells (RUCs) and subcells across an arbitrary number of length scales.

field quantities for any of the physics can also be determined by HFGMC (for example, the local heat fluxes and temperature gradients in the constituents throughout the composite). **Z** thus represents a general property tensor, while **Y** and **X** are the field variable vectors. Note that, for all the physics, the governing equation is given by,

$$\nabla \cdot \mathbf{Y} = 0 \tag{4}$$

In MsRM, see Figure 1, the scales are linked by equilibrating the homogenized fields and properties (global strain, stress, and stiffness tensors for the mechanical problem and global temperature gradient, heat flux, and thermal conductivity tensors for the thermal problem, for example) at level *i* to the analogous local fields and properties of a given sub-volume at level *i+1* (with appropriate transformation to account for the potential coordinate system change from scale to scale). Hence, starting with the lowest scale (*k*) microstructure (see Figure 1), whose sub-volumes contain only monolithic materials, the effective stiffness (**C**) or multiple physics property (**Z**) tensors can be calculated. This stiffness or property tensor (after appropriate coordinate transformation) then represents the homogenized material occupying one of the sub-volumes within a composite material at the next higher length scale. Given the transformed effective stiffness (**C**) or property (**Z**) tensors of all sub-volumes at this next higher length scale, the effective stiffness and property tensors of the composite at this level can be determined. These stiffness and property tensors can then be transformed and passed along to the next higher length scale, and the process repeats until the highest length scale considered (0) is reached.

As an example, for an MsRM analysis considering three length scales (0, 1, and 2), the overall effective stiffness tensor can be written as,

$$\mathbf{C}_0^* = \sum_{\alpha_0} v_{\alpha_0} \left\{ \left(\mathbf{T}_4^1\right)^{-1} \sum_{\alpha_1} v_{\alpha_1} \left[\left(\mathbf{T}_4^2\right)^{-1} \sum_{\alpha_2} v_{\alpha_2} \mathbf{C}_2^{(\alpha_2)} \mathbf{A}_2^{M(\alpha_2)} \right]^{(\alpha_1)} \mathbf{A}_1^{M(\alpha_1)} \right\}^{(\alpha_0)} \mathbf{A}_0^{M(\alpha_0)} \tag{5}$$

whereas the effective property tensor can be written as,

$$\mathbf{Z}_0^* = \sum_{\alpha_0} v_{\alpha_0} \left\{ \left(\mathbf{T}_2^1 \right)^{-1} \sum_{\alpha_1} v_{\alpha_1} \left[\left(\mathbf{T}_2^2 \right)^{-1} \sum_{\alpha_2} v_{\alpha_2} \mathbf{Z}_2^{(\alpha_2)} \mathbf{A}_2^{MP(\alpha_2)} \right]^{(\alpha_1)} \mathbf{A}_1^{MP(\alpha_1)} \right\}^{(\alpha_0)} \mathbf{A}_0^{MP(\alpha_0)} \tag{6}$$

Here, $\mathbf{A}_i^{M(\alpha_i)}$ and $\mathbf{A}_i^{MP(\alpha_i)}$ are the mechanical problem and multiple physics problem concentration tensors, respectively, which map the global applied fields to the local fields. $\mathbf{T}_2^i$ and $\mathbf{T}_4^i$ are the appropriate second and fourth order coordinate transformation matrices, v_{α_i} is the volume fraction of sub-volume α_i, and $\mathbf{C}_i^{(\alpha_i)}$ and $\mathbf{Z}_i^{(\alpha_i)}$ are the stiffness and property tensors of sub-volume α_i at level *i*. Note that in Equations (5) and (6), the superscript on the bracketed terms indicates that all variables within the brackets are a function of the sub-volume indices from the next higher length scale (including lower scale volume fractions and sub-volume indices). The intent of this notation is to fully define the sub-volume at a given scale as one progresses down the length scales. Note that multiscale localization equations for both the mechanical and multiphysics problems provide the field variable at any level (Ref. 25).

3.0 Multiscale Recursive Micromechanics Model for Semicrystalline Thermoplastics

3.1 Hierarchy of Multiscale Model

The hierarchy of the relevant length scales in the thermoplastic is depicted in Figure 2(a), and the geometry of the associated micromechanics models are shown in Figure 2(b). In Figure 2(a), the crystallite and amorphous constituents are represented in blue and peach, respectively. Four disparate length scales, Levels 0 (highest) – 3 (lowest), were explicitly considered. Within the MsRM (e.g., Eqs. (5) and (6)), the appropriate transformations were performed to ensure that the x^i-y^i-z^i coordinates (see Figure 2(b)) are aligned across the scales, where the superscript *i* indicates the scale at which the coordinate system operates. The thermoelastic properties of the crystallite and amorphous phases (Level 3) were calculated using MD, see Section 3.2 (Refs. 18 and 27). These properties were then used as the input for Level 2. The thermoelastic property calculations at the continuum scales (lamella/Level 2, lamellae stacks/Level 1, and spherulite/Level 0) were fully coupled using MsRM in NASMAT. GMC was used to model the granular crystalline blocks (GCBs), within Level 2, using two subcells by two subcells (2 x 2), doubly periodic, RUCs containing a crystallite subcell (blue) surrounded by three amorphous subcells (peach). The effective properties of the lamellae were computed through homogenization of the GCB. The lamellae stacks (Level 1) were also modeled with 2 x 2, doubly periodic, RUCs containing a single subcell utilizing the homogenized properties of the lamella from Level 2 and 3 amorphous subcells. In turn, the effective homogenized properties of Level 1 were used as subcell properties within the spherulite at Level 0.

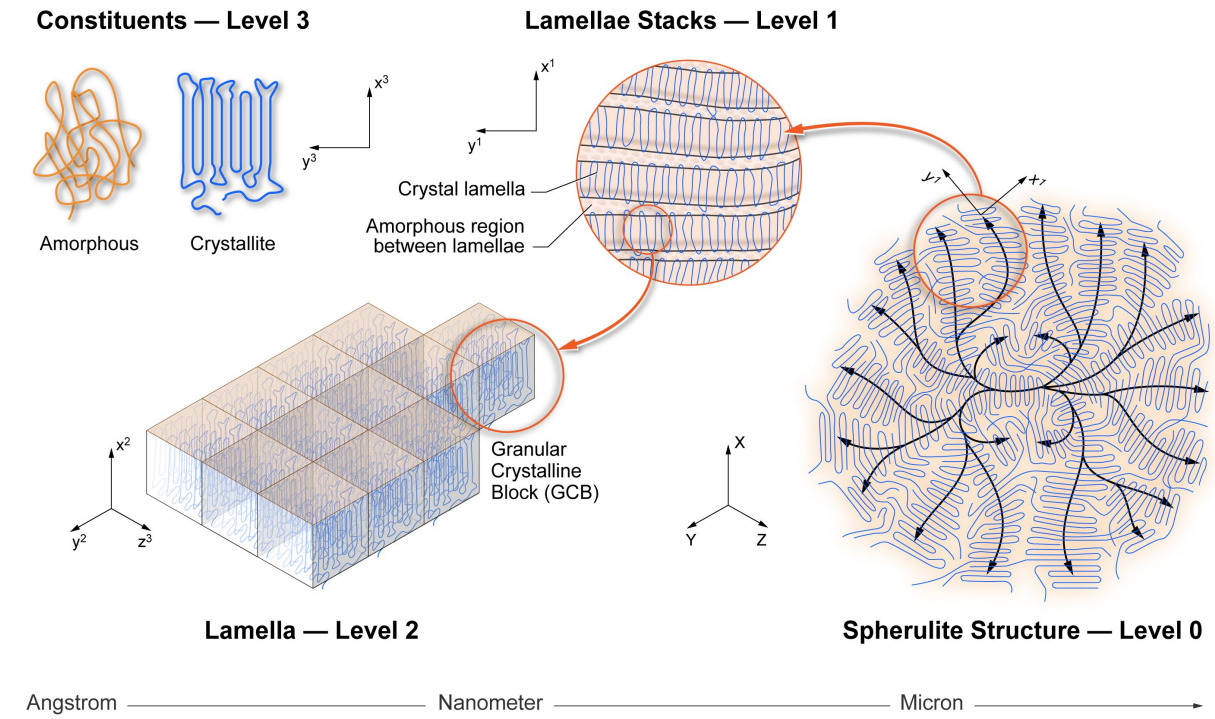

(a)

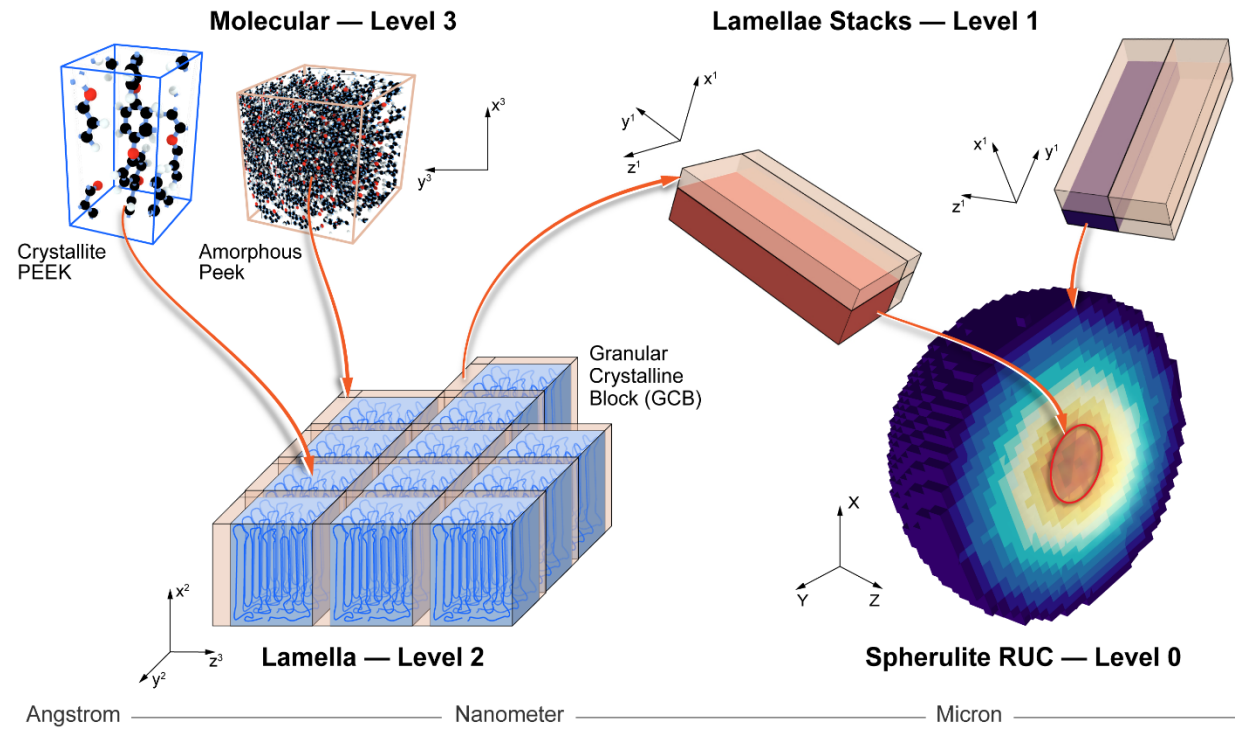

(b)

Figure 2.—Hierarchy of relevant length scales (constituent (phase), lamella, lamellae stacks, and spherulite) present in a semicrystalline thermoplastic. (a) Geometric idealizations. (b) Geometry used in micromechanics models.

TABLE I.—SUMMARY OF MsRM MODELS

Materials	Shape of Spherulite	Level 0 Micromechanics Theory
PEEK/PEKK	Sphere	GMC
PEEK/PEKK	Sphere	HFGMC
PEEK/PEKK	Cube	GMC
PEEK/PEKK	Cube	HFGMC

During solidification of the thermoplastic, the lamellae stacks in the spherulite grow radially outward from a nucleation site as the material is held at the crystallization temperature. The spherulites exist in an amorphous matrix phase which also occupies the volume between the lamella stacks. The amount of inter-spherulite matrix is dependent on how long the material is held at the crystallization temperature (Ref. 32). Manufacturing processes, such as annealing and quenching, may be utilized to affect the overall crystallinity and morphology. To predict the thermoelastic properties as function of the material microstructure accurately, it is important that the local crystallinity within the domain of the spherulite v_c and the overall crystallinity χ are approximated well in the multiscale model.

Seminal work in the development of this multiscale modeling strategy utilized triply periodic GMC at Level 0 to model the spherulite and assumed a pseudo cubic spherulite shape (Refs. 18 and 32). This strategy works well for predicting effective properties and is relatively insensitive to the shape of the spherulite due to the lack of normal-shear coupling inherent in GMC. However, with an eye towards predicting material nonlinearity, the current work also utilizes triply periodic HFGMC to perform the homogenization at Level 0, but with an added computational expense. The normal-shear coupling retained with HFGMC will introduce stress concentrations at the sharp corners of the cube, similar to FEM. Thus, the inclusion was also modeled as a voxelized sphere, as shown in Figure 2(b). For consistency, an MsRM model containing a spherical spherulite analyzed with GMC was also considered. A summary of the models presented in the work is given in Table I.

A unique aspect of the employed multiscale approach is its ability to capture the gradient in crystallinity within the spherulite. Because the crystallinity is denser within the core of the spherulites (Figure 2(b)), as opposed to near the perimeter, the Level 1 RUCs that were coupled to the Level 0 subcells near the core were assigned a lower volume fraction of amorphous subcells. This is depicted in Figure 2(b) using a color gradient within the spherulite at Level 0. Two example RUCs for the lamellae stacks are shown at Level 1 containing subcells colored to the corresponding colors of the parent subcells at Level 0 (e.g., red and blue). Moreover, the relative volume fractions of the lamellae within the lamellae stacks display the increased density of the lamellae near the core of the spherulite.

To achieve this gradient in crystallinity for the spherical model, it was assumed the core of the spherulite has a local crystallinity of 0.85, which was estimated based upon the 0.862 crystallinity of the GCB (Ref. 18). Then, the density of the lamellae stacks decreases in subcells as the radial distance from the center of the RUC increases, effectively controlling the local crystalline volume fraction v_c. The volume fraction of the lamellae subcells in the lamellae stacks (Level 1) are optimized to ensure the correct overall v_c, while the correct orientation of the lamellae stacks that form the spherulite is also ensured. Figure 3 shows the algorithm used to generate the MsRM model and write the NASMAT input file for the spherical model. The cubic model is based upon previous work. For details on that algorithm, the reader is referred to Reference 18.

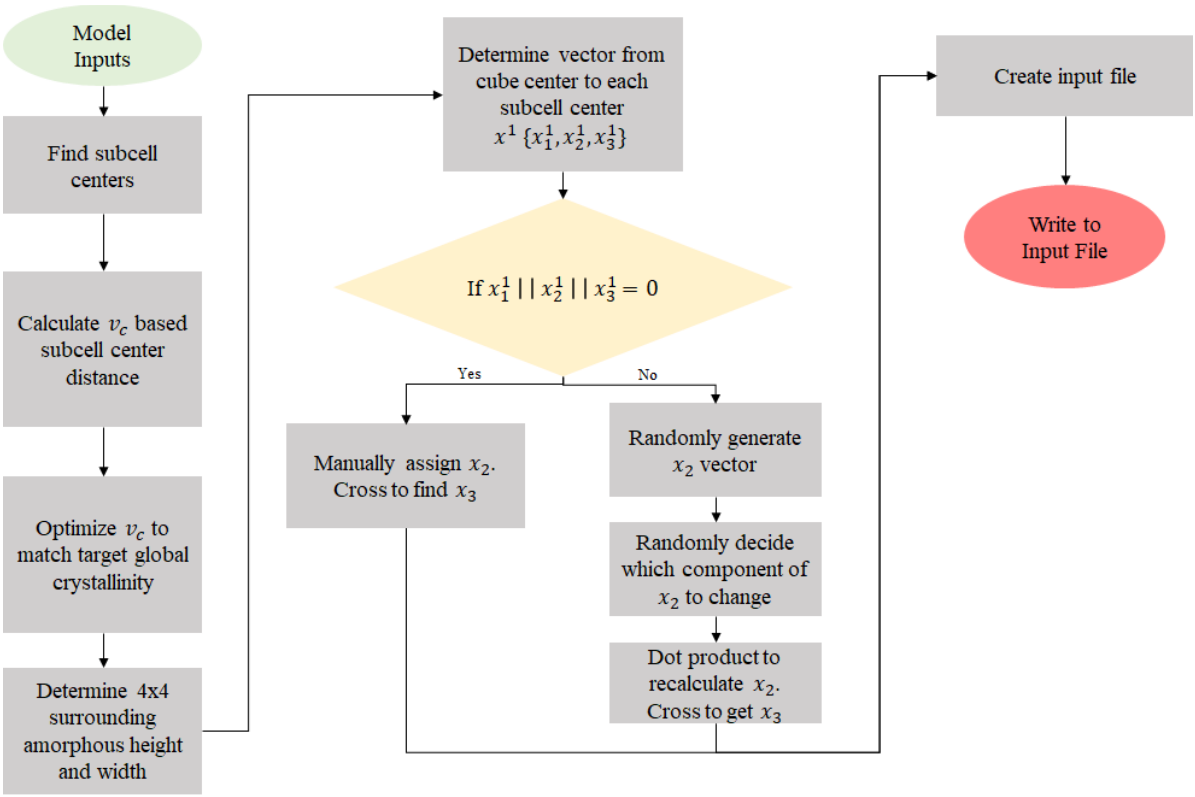

Figure 3.—Algorithm for constructing the MsRM model and writing the NASMAT input file.

3.2 Modeling Inputs

The thermoelastic constituent properties (amorphous and crystalline phases) of the models were obtained from MD simulations at room temperature and used in the continuum MsRM models as the primary material parameter inputs. The PEEK properties were averaged from statistical data calculated using MD (Ref. 18). Values for Young's modulus E_a, shear modulus G_a, and Poisson's ratio v_a of the amorphous phase of PEEK are presented in Table II. Note, the results from the MD simulations are stochastic and not necessarily isotropic. The data in Table II represents the average values of the Young's modulus, shear modulus, and Poisson's ratio from all the MD simulations. The average orthotropic properties of the crystalline PEEK (Young's modulus E_{ii}, shear modulus G_{ij}, and Poisson's ratio v_{ij}) are given in Table III. The subscripts i, j represent the direction at Level 3 (see Figure 2, x^3, y^3, z^3).

More recently, properties of PEKK 7002 were predicted with MD, which has a terephthalic acid (T) or isophthalic acid (I) ratio of 70/30 (Ref. 27). The average amorphous values are given in Table IV including the CTE α_a and thermal conductivity κ_a. Unlike PEEK, crystalline PEKK can exist in various forms, i.e., Form 1, Form 2i, and Form 2ii which are described and modeled with MD in Kemppainen et al. (Ref. 27). Since it was uncertain what crystalline forms existed in the material used to produce the data for validation, the averages of values (see Table III) for the properties of the different forms are used in the predictions here (Ref. 3). Only the longitudinal values of thermal conductivity κ_{xx} for the crystalline PEKK unit cells were calculated using MD (Ref. 27). Since thermal conductivity is affected by bond stiffness and van der Waals interactions, the thermal conductivity in transverse directions κ_{yy}, κ_{zz} in Table IV was estimated by scaling the longitudinal thermal conductivity κ_{xx} by the ratio of the stiffnesses E_{yy}/E_{zz}. The CTE in Table IV was calculated as a volumetric quantity; so, the same value is used for all directions in the crystalline PEKK.

TABLE II.—THERMOELASTIC CONSTITUENT PROPERTIES OF AMORPHOUS PEEK AND PEKK OBTAINED FROM MD (REFS. 18, 19, AND 27)

Property	PEEK	PEKK
E_a (GPa)	3.62 (Ref. 18)	3.20 (Ref. 27)
G_a (GPa)	1.28 (Ref. 18)	1.09 (Ref. 27)
ν_a	0.38 (Ref. 18)	0.44 (Ref. 27)
α_a (1/°C)	6.07E-5 (Ref. 19)	5.59E-5 (Ref. 27)
κ_a (W/(m-K))	----------	0.43 (Ref. 27)

TABLE III.—ELASTIC CONSTITUENT PROPERTIES OF CRYSTALLINE PEEK AND PEKK OBTAINED FROM MD (REFS. 18 AND 27)

Property	PEEK (Ref. 18)	PEKK (Ref. 27)
E_{xx} (GPa)	117.0	137.1
E_{yy} (GPa)	8.51	3.23
E_{zz} (GPa)	8.37	3.81
G_{yz} (GPa)	1.52	3.33
G_{xz} (GPa)	1.4	3.39
G_{xy} (GPa)	0.89	2.08
ν_{yz}	0.5	0.41
ν_{xz}	1.92	0.11
ν_{xy}	0.69	0.54

TABLE IV.—AVERAGED THERMOELASTIC CONSTITUENT PROPERTIES OF THE DIFFERENT FORMS CRYSTALLINE PEEK AND PEKK (REFS. 19 AND 27)

Thermal Property	α_{xx} (1/°C)	α_{yy} (1/°C)	α_{zz} (1/°C)	κ_{xx} (W/(m-K))	κ_{yy} (W/(m-K))	κ_{zz} (W/(m-K))
PEEK (Ref. 19)	4.29E-5	1.44E-4	–7.33E-6	----------	----------	----------
PEKK (Ref. 27)	8.52E-5	8.52E-5	8.52E-5	2.80	0.049	0.049

4.0 Prediction of Thermoelastic Properties as a Function of Crystallinity

The thermoelastic properties as a function of crystallinity for PEEK and PEKK, predicted with the four models described in Table I using NASMAT and discretized at the highest scale, based on a convergence study, with 32 x 32 x 32 subcells are presented in this section. Experimental data available in the open literature on these materials is extremely limited, but the computational results have been compared to experiments when available.

The effective Young's modulus E predicted as a function of χ is shown in Figure 4 for PEEK and PEKK. All models show excellent agreement with the test data (Refs. 2 and 3). The HFGMC models predictions exhibit a slightly stiffer response than GMC and tend to be more accurate with an increase in crystallinity. Moreover, the HFGMC results exhibit a convex behavior similar with the experimental data. In Figure 4(a), all models predict a higher modulus than the single experimental data point at a crystallinity of 0.16. However, this data falls within the experimental scatter presented in Reference 2. The shape of the geometry of the spherulite seems to have minimal influence on the Young's modulus. This indicates it is primarily influenced by the crystallinity, and not the geometry, of the spherulite. Further studies are needed to understand the effects on spherulite packing and morphology. The predictions for the Young's modulus of PEKK are plotted against the experimental data in Figure 4(b) and are in very good agreement. Note, the experimental data presented in Figure 4(b) is an amalgamation of data for three different forms of PEKK (6002, 7002, 8002), whereas the predictions strictly utilized properties predicted for PEKK 7002. The same discrepancies and trends among the GMC and HFGMC models, with the different geometries, are observed in the predictions for PEKK as for PEEK. Differences between the predictions of HFGMC and GMC of the observed magnitude and trend are expected due to the mismatches in properties between the crystalline and amorphous phases, along with the fact that the microstructure is discontinuous. It is well established that the first-order nature of GMC renders its predictions more approximate under such conditions (Ref. 22).

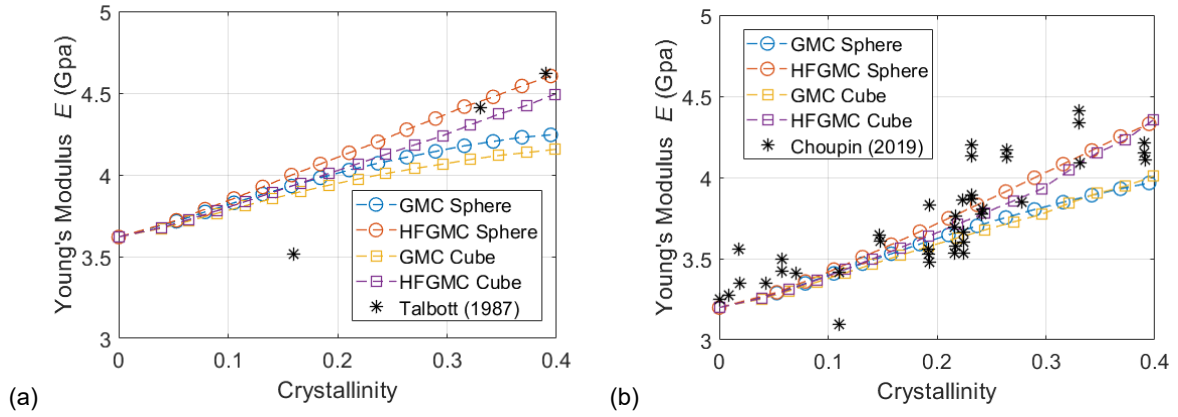

Figure 4.—Predicted effective Young's modulus as a function of crystallinity compared to available experimental data (Refs. 2 and 3). (a) PEEK. (b) PEKK.

Figure 5 shows the predictions for the effective shear modulus G of PEEK and PEKK. Only limited experimental data was available for PEEK and shown in Figure 5(a). Both models slightly over predict the experimental shear stiffness; again with, HFGMC predicting slightly higher shear moduli than GMC. No experimental data for the shear modulus of PEKK was obtained.

Predictions of the Poisson's ratios ν of PEEK and PEKK as a function of crystallinity are plotted in Figure 6. No experimental data was found for ν in the literature. The micromechanics theory used at Level 0 had only a slight effect on predictions for the Poisson's ratio. The trend predicted for PEEK and PEKK are opposite which can be attributed to the large ν_{xz} value predicted for crystalline PEEK with MD (Ref. 18) (see Table IV).

Available experimental data for the thermal properties is even more limited in the literature. Figure 7(a) shows the predicted CTE for PEEK as a function of crystallinity compared to experimental data (Refs. 34 and 35). The models exhibited between ~18 to 27 percent error compared to Reference 35 at 0 and ~0.35 crystallinity. However, the predicted trends match the data reasonably, especially from HFGMC, where the CTE slightly increased up to ~0.18 crystallinity and then decreased with an increase in crystallinity. The predictions were in better agreement (< 2 percent) with the more recent data for the CTE

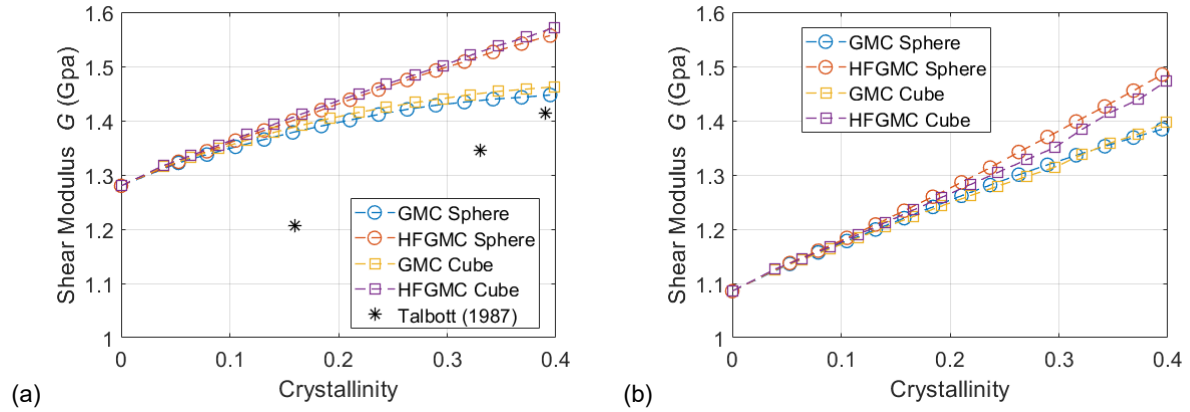

Figure 5.—Predicted effective shear modulus as a function of crystallinity compared to available experimental data (Ref. 2). (a) PEEK. (b) PEKK.

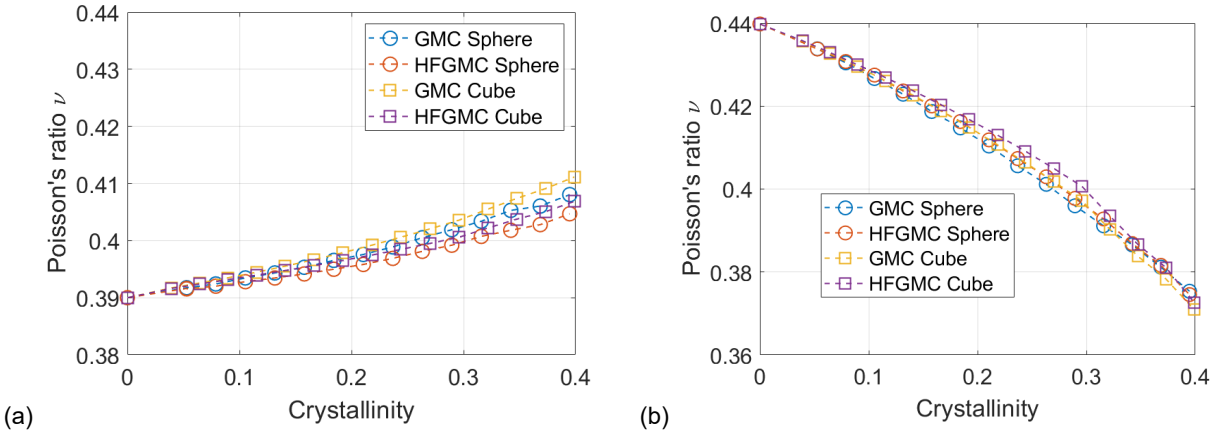

Figure 6.—Predicted effective Poisson's ratio as a function of crystallinity. (a) PEEK. (b) PEKK.

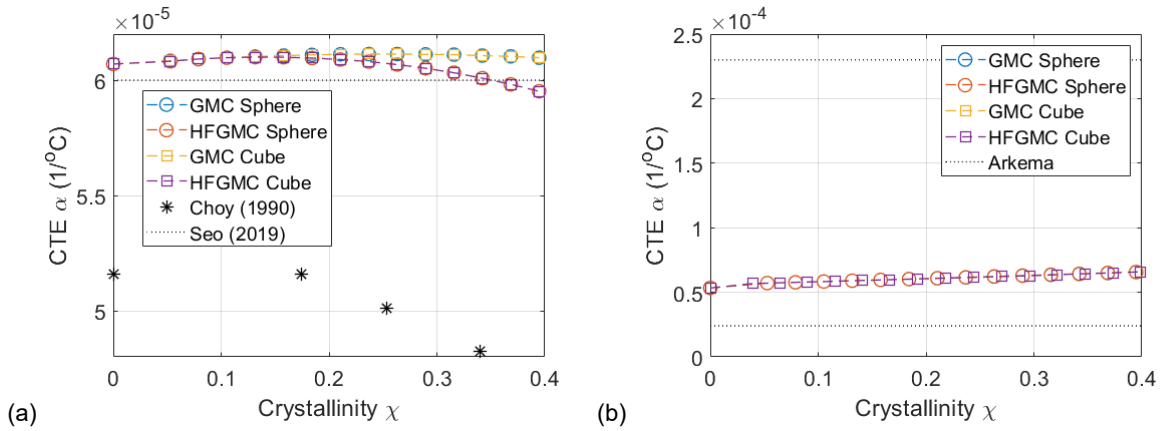

Figure 7.—Predicted effective CTE as a function of crystallinity compared to experimental data (Refs. 33 to 36). (a) PEEK. (b) PEKK. Experimental data average values measured from –100 °C to T_g and T_g to 300 °C.

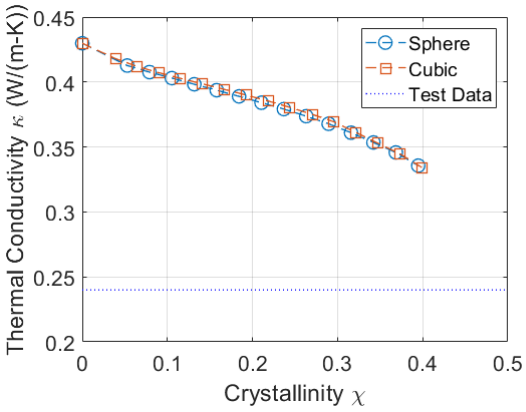

Figure 8.—Predicted effective thermal conductivity as a function of crystallinity for PEKK compared to experimental data with an unspecified crystallinity (Ref. 37).

given by Seo (Ref. 35). However, crystallinity was not reported in Reference 35. The experimental data for PEKK was obtained from a datasheet produced by Arkema which did not list the crystallinity of the material (Ref. 34). Moreover, this data was presented as two values: the average of measurements taken between (1) –100 °C to T_g and (2) T_g to 300 °C. That said, the modeling predictions are bounded by the two data points. The PEKK simulation results are only sensitive to the crystallinity, not the morphology, because an isotropic volumetric CTE was used as input (Ref. 27). For both materials the predicted influence of crystallinity on the CTE is small, which is consistent with previous predictions from a multiscale model for PEEK (Ref. 19).

Finally, the predictions for the effective thermal conductivity κ as a function of crystallinity are given in Figure 8 for PEKK. Note that only the HFGMC multiphysics micromechanics have been implemented in NASMAT. Therefore, the results in Figure 8 were generated using the HFGMC method at every scale. Experimental data available in the open literature for thermal conductivity of PEKK is extremely sparse,

and none was obtained for PEEK. The thermal conductivity of PEKK was reported as 2.4 W/(m-K), but no information on crystallinity or crystalline forms was given (Ref. 34). The predictions are considerably higher than this value. The shape of the spherulite had a minimal effect on the predicted effective thermal conductivity calculations, and the models predicted that conductivity decreases as crystallinity increases. This indicates that the κ_{yy} and κ_{zz} thermal conductivities of the crystalline phase, which are an order of magnitude smaller than the thermal conductivity of the amorphous phase, have a significant influence on the effective conductivity of the semicrystalline polymer. As mentioned in Section 3.2, these properties were estimated. Therefore, future efforts should be placed on calculating these properties using MD. More experimental data for both the CTE and thermal conductivity is needed before any conclusions can be drawn about the multiscale model thermal property predictions.

The following data are intended to provide some information on the computational demands of the presented multiscale models. The total number of subcells, across three scales, in each multiscale analysis was 16,384. Each analysis was run on a single processor of an Intel Xeon CPU E5-2698 v4 with 2.20 GHz per node. Analysis times ranged from ~40 to 180 sec, ~185 to 315 sec, ~90 to 220 sec for GMC, HFGMC, and vectorized HFGMC, respectively. As such, multistep simulations that include nonlinear effects such as damage, plasticity, and viscoelasticity are feasible.

5.0 Conclusion

A multiscale model for a single spherulite RUC was developed for semicrystalline thermoplastics within the MsRM framework implemented in NASMAT. Several models were evaluated by changing the shape of the spherulite inclusion (cubic and spherical) as well as the analysis methods used at the highest scale (GMC and HFGMC). Inputs for properties of the amorphous and crystalline phases used as the base constituents for the models were obtained from MD simulations. Therefore, the predictions presented here were obtained entirely using virtual data.

Model predictions of the thermoelastic properties of PEEK and PEKK as function of crystallinity were in good agreement with the limited experimental data available in the literature. In general, the models that utilized HFGMC at the highest scale predicted higher stiffness as the crystallinity was increased and tended to be more accurate with respect to the available experimental data. The effective properties were not substantially affected by the shape of the spherulite employed in the model. However, the HFGMC results would be affected by changes in the morphology of the microstructure. It is expected that accuracy in the local fields needed for non-linear predictions would be more sensitive to the micromechanics theory used. Test data on the CTE of thermoplastics PEEK and PEKK is very limited, but the modeling predictions were bounded by the data.

With the validated multiscale model in place, additional studies can be performed including sensitivity of the effective properties and local fields calculated through de-homogenization to morphological effects of the semicrystalline microstructure of thermoplastics, such as the packing of the spherulites and ratio of inter-spherulite amorphous matrix to crystalline phases. Damage and inelastic material models can be employed at the constituent scales and used to predict the nonlinear behavior of the thermoplastics. In addition, crystallization kinetics simulations can be used in conjunction with model to perform processing simulations (Ref. 37). Finally, this model can be integrated into a model for fibrous composites to perform multiscale simulations of fiber reinforced thermoplastic composites considering both the fiber architecture and matrix microstructure.

References

1. Pérez-Martín, H., Mackenzie, P., Baidak, A., Ó Brádaigh, C.M., and Ray, D. (2021). "Crystallinity Studies of PEKK and Carbon Fibre/PEKK Composites: A Review," *Composites Part B*, Vol. 223, 109127.
2. Talbott, M.F., Springer, G.S., and Berglund, L.A. (1987). "The Effects of Crystallinity on the Mechanical Properties of PEEK Polymer and Graphite Fiber Reinforced PEEK," *Journal of Composite Materials*, Vol. 21, pp. 1056–1080.
3. Choupin, T., Debertrand, L., Fayolle, B., Régnier, G., Paris, C., Cinquin, J., and Brulé, B. (2019). "Influence of thermal history on the mechanical properties of poly(ether ketone ketone) copolymers," *Polymer Crystallization*, 2(6), pp. 1–8.
4. Bandyopadhyay, A., Valavala, P.K., Clancy, T.C., Wise, K.E., and Odegard, G.M. (2011). "Molecular Modeling of Crosslinked Epoxy Polymers: The Effect of Crosslink Density on Thermomechanical Properties," *Polymer*, Vol. 52, No. 11, pp. 2334–2452.
5. Odegard, G.M., Jensen, B.D., Gowtham, S., Wu, J., He, J., and Zhang, Z. (2014). "Predicted mechanical response of crosslinked epoxy using ReaxFF," *Chemical Physics Letters*, pp. 175–178.
6. Chapman, T.J., Gillespie, Jr., J.W., Pipes, R.B., Manson, J.-A. E., and Seferis, J.C., "Prediction of Process-Induced Residual Stresses in Thermoplastic Composites," *Journal of Composite Materials*, 24, 1990, pp. 616–643.
7. Ogale, A.A. and McCullough, R.L. "Influence of microstructure on elastic and viscoelastic properties of polyether ether ketone," *Composite Science and Technology*, 30, 1987, pp. 185–201.
8. Guan, X. and Pitchumani, R. "A Micromechanical Model for the Elastic Properties of Semicrystalline Thermoplastic Polymers," *Polymer Engineering and Science*, 44, 2004, pp. 433–451.
9. Bédoui, F., Diani, J., Régnier, G., and Seiler, W. "Micromechanical modeling of isotropic elastic behavior of semicrystalline polymers," *Acta Materialia*, 54, 2006, pp. 1513–1523.
10. Diani, J., Bédoui, F., and Régnier, G. "On the relevance of the micromechanics approach for predicting the linear viscoelastic behavior of semi-crystalline poly(ethylene)terephtalates (PET)" *Materials Science and Engineering A*, 475, 2008, pp. 229–234.
11. Gueguen, O., Ahzi, S., Belouettar, S., and Makradi, A. "Comparison of micromechanical models for the prediction of the effective elastic properties of semicrystalline polymers: Application to polyethylene," *Polymer Science Series A*, 50, 2008, pp. 523–532.
12. Glüge, R., Altenbach, H., Kolesov, I., Mahmood, N., Beiner, M., and Androsch, R. "On the effective elastic properties of isotactic polypropylene," *Polymer*, 160, 2019, pp. 291–302.
13. van Dommelen, J.A.W., Poluektov, M., Sedighiamiri, A., and Govaert, L.E. "Micromechanics of semicrystalline polymers: Towards quantitative predictions," *Mechanics Research Communications*, 80, 2017, pp. 4–9.
14. Hsia, K.J, Xin, Y.B., and Lin, L. "Numerical simulation of semi-crystalline nylon 6: elastic constants of crystalline and amorphous parts," *J. Mater. Sci.*, 29, 1994, 1601–1611.
15. Doyle, M.J. "On the effect of crystallinity on the elastic properties of semicrystalline polyethylene," *Polym. Eng. Sci.*, 40, 2000, pp. 330–335.
16. Poluektov, M., van Dommelen, J.A.W., Govaert, L.E., Yakimets, I., and Geers, M.G.D. "Micromechanical modelling of poly(ethylene terephthalate) using a layered two-phase approach," *J. Mater. Sci.*, 48, 2013, pp. 3769–3781.
17. Jin, L. Ball, J., Bremner, T., and Sue, H.-J. "Crystallization behavior and morphological characterization of poly(ether ether ketone)," *Polymer*, 55, 2014, pp. 5255–5265.

18. Pisani, W.A., Radue, M.S., Chinkanjanarot, S., Bednarcyk, B.A., Pineda, E.J., Waters, K., Pandey, R., King, J.A., and Odegard, G.M. (2019). "Multiscale Modelling of PEEK using Reactive Molecular Dynamics Modeling and Micromechanics," *Polymer*, Vol. 163, pp. 96–105.
19. Kashmari, K., Deshpande, P., Patil, S., Maiaru, M., and Odegard, G.M. (2022). "A multiscale approach to investigate the effect of temperature and crystallinity on the development of residual stresses in semicrystalline PEEK," *American Society for Composites 37th Technical Conference*, 19–21 September, Tucson, AZ.
20. van Duin, A.C.T., Dasgupta, S., Lorant, F., and Goddard, W.A. (2001). "ReaxFF: A Reactive Force Field for Hydrocarbons," *The Journal of Physical Chemistry A*, Vol. 105, No. 41, pp. 9393–9409.
21. Bednarcyk, B.A., and Arnold, S.M. (2002). "MAC/GMC 4.0 User's Manual - Keywords Manual," *NASA TM-2002-212077/Vol2*.
22. Aboudi, J., Arnold, S.M., and Bednarcyk, B.A. (2013). *Micromechanics of Composite Materials: A Generalized Multiscale Analysis Approach*, Oxford, UK: Elsevier.
23. Pisani, W.A., Newman, J.K., and Shukla, M.K. (2021). "Multiscale Modeling of Polyamide 6 Using Molecular Dynamics and Micromechanics," *Industrial & Engineering Chemistry Research*, Vol. 60, No. 37, pp. 13604–13613.
24. Bednarcyk, B.A., Pineda, E.J., Ricks, T.M., and Mital, S.K. (2021). "Progressive Damage Response of 3D Woven Composites via the Multiscale Recursive Micromechanics Solution with Tailored Fidelity," *American Society for Composites 36th Technical Conference*, 20-22 September 2021, Virtual Conference.
25. Pineda, E.J., Bednarcyk, B.A., Ricks, T.M., and Henson, G. (2021). "Efficient Multiscale Recursive Micromechanics of Composites for Engineering Applications," *International Journal for Multiscale Computational Engineering*, 19(4), 77–105.
26. Bednarcyk, B.A., Aboudi, J., and Arnold, S.M., (2017). "Micromechanics of composite materials governed by vector constitutive laws," *International Journal of Solids and Structures*, Vol. 110–111, pp. 137–151.
27. Kemppainen, J.D., Varshney, V., Pineda, E.J., and Odegard, G.M. (2022). Thermo-mechanical property prediction of amorphous/crystal PEKK via molecular dynamics. NASA-TM-20220018678.
28. Pineda, E.J., Bednarcyk, B.A., Ricks, T.M., Farrokh, B., and Jackson, W.C. (2022). "Multiscale Failure Analysis of a 3D Woven Composite Containing Manufacturing Voids and Disbonds," *Composites Part A: Applied Science and Manufacturing*, 156(2022) 106844.
29. Bednarcyk, B.A., Ricks, T.M., Pineda, E.J., Murthy, P., Mital, S., Hu, Z., and Gustafson, P.A. (2022). "Thermal Conductivity of 3D Woven Composite Thermal Protection System Materials via Multiscale Recursive Micromechanics," *2022 AIAA SciTech Forum*, 3-7 January 2022, San Diego, CA.
30. Ricks, T.M., Pineda, E.J., Bednarcyk, B.A., and Arnold, S.M. (2021) "Progressive Failure Analysis of 3D Woven Composites via Multiscale Recursive Micromechanics," *AIAA SciTech Forum* (virtual), Jan. 11-21, 10.2514/6.2021-0702.
31. Pahr, D., and Arnold, S.M. (2002). "The applicability of the generalized method of cell for analyzing discontinuously reinforced composites," *Composites Part B: Engineering*, 33 (2), pp. 153–170.
32. Choupin, T., Fayolle, B., Régnier, G., Paris, C., Cinquin, J., and Brulé, B. (2017). "Isothermal crystallization kinetic modeling of poly(etherketoneketone) (PEKK) copolymer," *Polymer*, 111, pp. 73–82.
33. Arkema. (2012). KEPSTAN by Arkema Technical Data – 7000 Series.
34. Choy, C.L., Leung, W.P., and Nakafuku, C. (1990). "Thermal expansion of poly (ether-ether- ketone) (PEEK)," *Journal of Polymer Science: Part B: Polymer Physics*, 28, pp. 1965–1977.

35. Seo, J., Gohn, A.M., Dubin, O., Takahashi, H., Hasegawa, H., Sato, R., Rhoades, A.M., Schaake, R.P., and Colby, Ralph H. (2019). “Isothermal crystallization of poly(ether ether ketone) with different molecular weights over a wide temperature range,” *Polymer Crystallization*, 2(1), e10055.
36. Polyetherketoneketone (PEKK) datasheet. (2022). https://matmatch.com/materials/mbas044-polyetherketoneketone-pekk-.\
37. Husseini, J.F., Pineda, E.J., and Stapleton, S.E. (2024). An algorithm for modeling thermoplastics spherulite growth using crystallization kinetics. *Materials*, 17(14), 3441.